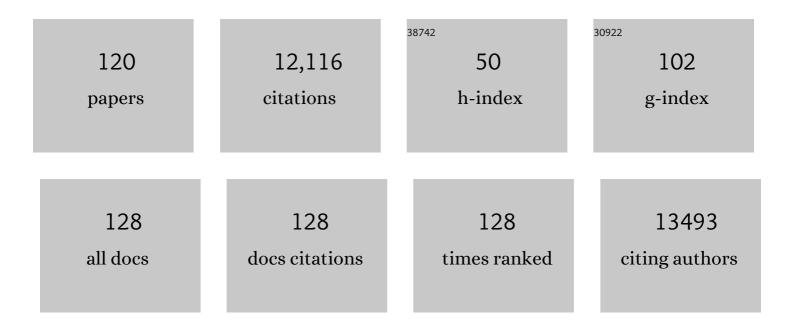
Thomas T Liu

List of Publications by Year in descending order

Source: https://exaly.com/author-pdf/3343086/publications.pdf Version: 2024-02-01



ΤΗΟΜΛς ΤΙΠ

#	Article	IF	CITATIONS
1	The Effects of Nicotine and Cannabis Co-Use During Late Adolescence on White Matter Fiber Tract Microstructure. Journal of Studies on Alcohol and Drugs, 2022, 83, 287-295.	1.0	7
2	Effects of Sub-threshold Transcutaneous Auricular Vagus Nerve Stimulation on Cingulate Cortex and Insula Resting-state Functional Connectivity. Frontiers in Human Neuroscience, 2022, 16, 862443.	2.0	5
3	The Effects of Nicotine and Cannabis Co-Use During Late Adolescence on White Matter Fiber Tract Microstructure Journal of Studies on Alcohol and Drugs, 2022, 83, 287-295.	1.0	Ο
4	A geometric view of signal sensitivity metrics in multi-echo fMRI. NeuroImage, 2022, 259, 119409.	4.2	1
5	Functional connectome fingerprinting using shallow feedforward neural networks. Proceedings of the National Academy of Sciences of the United States of America, 2021, 118, .	7.1	9
6	Defining Hypoperfusion in Chronic Aphasia: An Individualized Thresholding Approach. Brain Sciences, 2021, 11, 491.	2.3	9
7	070 Respiratory, cardiac, EEG, BOLD signals and functional connectivity over multiple microsleep episodes. Sleep, 2021, 44, A29-A29.	1.1	0
8	Respiratory, cardiac, EEG, BOLD signals and functional connectivity over multiple microsleep episodes. NeuroImage, 2021, 237, 118129.	4.2	13
9	Effects of sub-threshold transcutaneous auricular vagus nerve stimulation on cerebral blood flow. Scientific Reports, 2021, 11, 24018.	3.3	4
10	MRI in systems medicine. Wiley Interdisciplinary Reviews: Systems Biology and Medicine, 2020, 12, e1463.	6.6	4
11	Atypical Relationships Between Spontaneous EEG and fMRI Activity in Autism. Brain Connectivity, 2020, 10, 18-28.	1.7	21
12	Anterior Cingulate Structure and Perfusion is Associated with Cerebrospinal Fluid Tau among Cognitively Normal Older Adult APOE É>4 Carriers. Journal of Alzheimer's Disease, 2020, 73, 87-101.	2.6	5
13	Distinct thalamocortical network dynamics are associated with the pathophysiology of chronic low back pain. Nature Communications, 2020, 11, 3948.	12.8	59
14	The effects of nicotine and cannabis co-use during adolescence and young adulthood on white matter cerebral blood flow estimates. Psychopharmacology, 2020, 237, 3615-3624.	3.1	11
15	Interaction of APOE, cerebral blood flow, and cortical thickness in the entorhinal cortex predicts memory decline. Brain Imaging and Behavior, 2020, 14, 369-382.	2.1	8
16	Vigilance Effects in Resting-State fMRI. Frontiers in Neuroscience, 2020, 14, 321.	2.8	31
17	Dose-dependent association of accelerometer-measured physical activity and sedentary time with brain perfusion in aging. Experimental Gerontology, 2019, 125, 110679.	2.8	28
18	Nuisance effects in inter-scan functional connectivity estimates before and after nuisance regression. Neurolmage, 2019, 202, 116005.	4.2	3

#	Article	IF	CITATIONS
19	APOE modifies the interaction of entorhinal cerebral blood flow and cortical thickness on memory function in cognitively normal older adults. NeuroImage, 2019, 202, 116162.	4.2	22
20	Transient states of network connectivity are atypical in autism: A dynamic functional connectivity study. Human Brain Mapping, 2019, 40, 2377-2389.	3.6	61
21	Nuisance effects and the limitations of nuisance regression in dynamic functional connectivity fMRI. Neurolmage, 2019, 184, 1005-1031.	4.2	24
22	Awake Mouse Imaging: From Two-Photon Microscopy to Blood Oxygen Level–Dependent Functional Magnetic Resonance Imaging. Biological Psychiatry: Cognitive Neuroscience and Neuroimaging, 2019, 4, 533-542.	1.5	49
23	Template-based prediction of vigilance fluctuations in resting-state fMRI. NeuroImage, 2018, 174, 317-327.	4.2	65
24	Cerebral blood flow predicts differential neurotransmitter activity. Scientific Reports, 2018, 8, 4074.	3.3	78
25	The Effects of Global Signal Regression on Estimates of Resting-State Blood Oxygen-Level-Dependent Functional Magnetic Resonance Imaging and Electroencephalogram Vigilance Correlations. Brain Connectivity, 2018, 8, 618-627.	1.7	18
26	Reduced Regional Cerebral Blood Flow Relates to Poorer Cognition in Older Adults With Type 2 Diabetes. Frontiers in Aging Neuroscience, 2018, 10, 270.	3.4	83
27	Effects of HIV Infection, methamphetamine dependence and age on cortical thickness, area and volume. NeuroImage: Clinical, 2018, 20, 1044-1052.	2.7	24
28	Cerebral Blood Flow Measurements in Adults: A Review on the Effects of Dietary Factors and Exercise. Nutrients, 2018, 10, 530.	4.1	84
29	Rectified Gaussian Scale Mixtures and the Sparse Non-Negative Least Squares Problem. IEEE Transactions on Signal Processing, 2018, 66, 3124-3139.	5.3	15
30	Dynamic association between perfusion and white matter integrity across time since injury in Veterans with history of TBI. NeuroImage: Clinical, 2017, 14, 308-315.	2.7	31
31	Global signal regression acts as a temporal downweighting process in resting-state fMRI. NeuroImage, 2017, 152, 602-618.	4.2	53
32	The global signal in fMRI: Nuisance or Information?. NeuroImage, 2017, 150, 213-229.	4.2	339
33	Reprint of â€~Noise contributions to the fMRI signal: An Overview'. NeuroImage, 2017, 154, 4-14.	4.2	11
34	Dynamic functional connectivity in bipolar disorder is associated with executive function and processing speed: A preliminary study Neuropsychology, 2017, 31, 73-83.	1.3	89
35	Aberrant Cerebral Blood Flow in Response to Hunger and Satiety in Women Remitted from Anorexia Nervosa. Frontiers in Nutrition, 2017, 4, 32.	3.7	9
36	Short-term apparent brain tissue changes are contributed by cerebral blood flow alterations. PLoS ONE, 2017, 12, e0182182.	2.5	23

#	Article	IF	CITATIONS
37	Higher Brain Perfusion May Not Support Memory Functions in Cognitively Normal Carriers of the ApoE ε4 Allele Compared to Non-Carriers. Frontiers in Aging Neuroscience, 2016, 8, 151.	3.4	31
38	Noise contributions to the fMRI signal: An overview. NeuroImage, 2016, 143, 141-151.	4.2	227
39	The Cerebral Blood Flow Biomedical Informatics Research Network (CBFBIRN) data repository. NeuroImage, 2016, 124, 1202-1207.	4.2	5
40	Underconnected, But Not Broken? Dynamic Functional Connectivity MRI Shows Underconnectivity in Autism Is Linked to Increased Intra-Individual Variability Across Time. Brain Connectivity, 2016, 6, 403-414.	1.7	93
41	The Function Biomedical Informatics Research Network Data Repository. NeuroImage, 2016, 124, 1074-1079.	4.2	114
42	Differences in the resting-state fMRI global signal amplitude between the eyes open and eyes closed states are related to changes in EEG vigilance. NeuroImage, 2016, 124, 24-31.	4.2	107
43	Greater preference consistency during the Willingness-to-Pay task is related to higher resting state connectivity between the ventromedial prefrontal cortex and the ventral striatum. Brain Imaging and Behavior, 2016, 10, 730-738.	2.1	10
44	A pilot study investigating changes in neural processing after mindfulness training in elite athletes. Frontiers in Behavioral Neuroscience, 2015, 9, 229.	2.0	52
45	Elevated cerebrovascular resistance index is associated with cognitive dysfunction in the very-old. Alzheimer's Research and Therapy, 2015, 7, 3.	6.2	16
46	Temporal profile of brain response to alprazolam in patients with generalized anxiety disorder. Psychiatry Research - Neuroimaging, 2015, 233, 394-401.	1.8	20
47	Enhanced identification of BOLD-like components with multi-echo simultaneous multi-slice (MESMS) fMRI and multi-echo ICA. NeuroImage, 2015, 112, 43-51.	4.2	65
48	Increased Cerebral Blood Flow Associated with Better Response Inhibition in Bipolar Disorder. Journal of the International Neuropsychological Society, 2015, 21, 105-115.	1.8	19
49	Quality Assurance in Functional MRI. Biological Magnetic Resonance, 2015, , 245-270.	0.4	6
50	Interactive effects of vascular risk burden and advanced age on cerebral blood flow. Frontiers in Aging Neuroscience, 2014, 6, 159.	3.4	73
51	Game controller modification for fMRI hyperscanning experiments in a cooperative virtual reality environment. MethodsX, 2014, 1, 292-299.	1.6	6
52	Developmental changes in resting and functional cerebral blood flow and their relationship to the BOLD response. Human Brain Mapping, 2014, 35, 3188-3198.	3.6	17
53	MEG source imaging method using fast L1 minimum-norm and its applications to signals with brain noise and human resting-state source amplitude images. NeuroImage, 2014, 84, 585-604.	4.2	60
54	Increased Hippocampal Blood Flow in Sedentary Older Adults at Genetic Risk for Alzheimer's Disease. Journal of Alzheimer's Disease, 2014, 41, 809-817.	2.6	33

#	Article	IF	CITATIONS
55	Resting-State fMRI Activity Predicts Unsupervised Learning and Memory in an Immersive Virtual Reality Environment. PLoS ONE, 2014, 9, e109622.	2.5	26
56	A Survey of the Sources of Noise in fMRI. Psychometrika, 2013, 78, 396-416.	2.1	56
57	An Introduction to Normalization and Calibration Methods in Functional MRI. Psychometrika, 2013, 78, 308-321.	2.1	15
58	The amplitude of the resting-state fMRI global signal is related to EEG vigilance measures. NeuroImage, 2013, 83, 983-990.	4.2	248
59	Neurovascular factors in resting-state functional MRI. NeuroImage, 2013, 80, 339-348.	4.2	107
60	Altered Cerebral Perfusion in Executive, Affective, and Motor Networks During Adolescent Depression. Journal of the American Academy of Child and Adolescent Psychiatry, 2013, 52, 1076-1091.e2.	0.5	72
61	Interaction of Age and APOE Genotype on Cerebral Blood Flow at Rest. Journal of Alzheimer's Disease, 2013, 34, 921-935.	2.6	92
62	Cerebral blood flow response to acute hypoxic hypoxia. NMR in Biomedicine, 2013, 26, 1844-1852.	2.8	33
63	Resting-state fMRI activity in the basal ganglia predicts unsupervised learning performance in a virtual reality environment. , 2013, , .		2
64	High efficiency multishot interleaved spiralâ€∢i>in/out: Acquisition for highâ€resolution BOLD fMRI. Magnetic Resonance in Medicine, 2013, 70, 420-428.	3.0	6
65	Cortical and Subcortical Cerebrovascular Resistance Index in Mild Cognitive Impairment and Alzheimer's Disease. Journal of Alzheimer's Disease, 2013, 36, 689-698.	2.6	39
66	Caffeine-Induced Global Reductions in Resting-State BOLD Connectivity Reflect Widespread Decreases in MEG Connectivity. Frontiers in Human Neuroscience, 2013, 7, 63.	2.0	37
67	The Cerebral Blood Flow Biomedical Informatics Research Network (CBFBIRN) database and analysis pipeline for arterial spin labeling MRI data. Frontiers in Neuroinformatics, 2013, 7, 21.	2.5	20
68	Assessment of Alzheimer's Disease Risk with Functional Magnetic Resonance Imaging: An Arterial Spin Labeling Study. Journal of Alzheimer's Disease, 2012, 31, S59-S74.	2.6	73
69	A geometric view of global signal confounds in resting-state functional MRI. NeuroImage, 2012, 59, 2339-2348.	4.2	85
70	Caffeine increases the temporal variability of resting-state BOLD connectivity in the motor cortex. NeuroImage, 2012, 59, 2994-3002.	4.2	56
71	The development of event-related fMRI designs. NeuroImage, 2012, 62, 1157-1162.	4.2	31
72	An automatic MEG low-frequency source imaging approach for detecting injuries in mild and moderate TBI patients with blast and non-blast causes. NeuroImage, 2012, 61, 1067-1082	4.2	101

#	Article	IF	CITATIONS
73	Anti-correlated networks, global signal regression, and the effects of caffeine in resting-state functional MRI. NeuroImage, 2012, 63, 356-364.	4.2	130
74	Altered cerebral blood flow and neurocognitive correlates in adolescent cannabis users. Psychopharmacology, 2012, 222, 675-684.	3.1	65
75	Function biomedical informatics research network recommendations for prospective multicenter functional MRI studies. Journal of Magnetic Resonance Imaging, 2012, 36, 39-54.	3.4	201
76	On multiple alternating steady states induced by periodic spin phase perturbation waveforms. Magnetic Resonance in Medicine, 2012, 67, 1412-1418.	3.0	1
77	Pseudocontinuous arterial spin labeling with optimized tagging efficiency. Magnetic Resonance in Medicine, 2012, 68, 1135-1144.	3.0	36
78	Effect of Mild Cognitive Impairment and APOE Genotype on Resting Cerebral Blood Flow and its Association with Cognition. Journal of Cerebral Blood Flow and Metabolism, 2012, 32, 1589-1599.	4.3	65
79	Accurate reconstruction of temporal correlation for neuronal sources using the enhanced dual-core MEG beamformer. Neurolmage, 2011, 56, 1918-1928.	4.2	26
80	Adaptation of a Haptic Robot in a 3T fMRI. Journal of Visualized Experiments, 2011, , .	0.3	2
81	Alcohol Effects on Cerebral Blood Flow in Subjects With Low and High Responses to Alcohol. Alcoholism: Clinical and Experimental Research, 2011, 35, 1034-1040.	2.4	56
82	A novel method for quantifying scanner instability in fMRI. Magnetic Resonance in Medicine, 2011, 65, 1053-1061.	3.0	46
83	Multiphase pseudocontinuous arterial spin labeling (MPâ€PCASL) for robust quantification of cerebral blood flow. Magnetic Resonance in Medicine, 2010, 64, 799-810.	3.0	90
84	Cortical depth-specific microvascular dilation underlies laminar differences in blood oxygenation level-dependent functional MRI signal. Proceedings of the National Academy of Sciences of the United States of America, 2010, 107, 15246-15251.	7.1	267
85	An arterial spin labeling investigation of cerebral blood flow deficits in chronic stroke survivors. Neurolmage, 2010, 51, 995-1005.	4.2	62
86	Caffeine increases the linearity of the visual BOLD response. NeuroImage, 2010, 49, 2311-2317.	4.2	12
87	Differential age effects on cerebral blood flow and BOLD response to encoding: Associations with cognition and stroke risk. Neurobiology of Aging, 2009, 30, 1276-1287.	3.1	82
88	Cerebral perfusion and oxygenation differences in Alzheimer's disease risk. Neurobiology of Aging, 2009, 30, 1737-1748.	3.1	171
89	Inter-subject variability in hypercapnic normalization of the BOLD fMRI response. NeuroImage, 2009, 45, 420-430.	4.2	50
90	Caffeine reduces resting-state BOLD functional connectivity in the motor cortex. NeuroImage, 2009, 46, 56-63.	4.2	69

#	Article	IF	CITATIONS
91	Optimal phase difference reconstruction: comparison of two methods. Magnetic Resonance Imaging, 2008, 26, 142-145.	1.8	24
92	Imaging periodic currents using alternating balanced steadyâ€state free precession. Magnetic Resonance in Medicine, 2008, 59, 140-148.	3.0	21
93	Noninvasive measurement of the cerebral blood flow response in human lateral geniculate nucleus with arterial spin labeling fMRI. Human Brain Mapping, 2008, 29, 1207-1214.	3.6	10
94	SNR and functional sensitivity of BOLD and perfusion-based fMRI using arterial spin labeling with spiral SENSE at 3 T. Magnetic Resonance Imaging, 2008, 26, 513-522.	1.8	27
95	Caffeine-induced uncoupling of cerebral blood flow and oxygen metabolism: A calibrated BOLD fMRI study. NeuroImage, 2008, 40, 237-247.	4.2	148
96	Calibrated fMRI in the medial temporal lobe during a memory-encoding task. NeuroImage, 2008, 40, 1495-1502.	4.2	32
97	Caffeine reduces the activation extent and contrast-to-noise ratio of the functional cerebral blood flow response but not the BOLD response. NeuroImage, 2008, 42, 296-305.	4.2	54
98	Measurement of cerebral perfusion with arterial spin labeling: Part 2. Applications. Journal of the International Neuropsychological Society, 2007, 13, 526-38.	1.8	93
99	Measurement of cerebral perfusion with arterial spin labeling: Part 1. Methods. Journal of the International Neuropsychological Society, 2007, 13, 517-25.	1.8	173
100	A component based noise correction method (CompCor) for BOLD and perfusion based fMRI. NeuroImage, 2007, 37, 90-101.	4.2	3,466
101	Cerebral blood flow and BOLD responses to a memory encoding task: A comparison between healthy young and elderly adults. NeuroImage, 2007, 37, 430-439.	4.2	99
102	A Primer on Functional Magnetic Resonance Imaging. Neuropsychology Review, 2007, 17, 107-125.	4.9	59
103	Physiological noise reduction for arterial spin labeling functional MRI. NeuroImage, 2006, 31, 1104-1115.	4.2	100
104	Caffeine reduces the initial dip in the visual BOLD response at 3 T. NeuroImage, 2006, 32, 9-15.	4.2	49
105	Velocity-selective arterial spin labeling. Magnetic Resonance in Medicine, 2006, 55, 1334-1341.	3.0	224
106	Bayesian inference of hemodynamic changes in functional arterial spin labeling data. Magnetic Resonance in Medicine, 2006, 56, 891-906.	3.0	39
107	A signal processing model for arterial spin labeling functional MRI. NeuroImage, 2005, 24, 207-215.	4.2	202
108	An arteriolar compliance model of the cerebral blood flow response to neural stimulus. NeuroImage, 2005. 25. 1100-1111.	4.2	124

#	Article	IF	CITATIONS
109	Discrepancies between BOLD and flow dynamics in primary and supplementary motor areas: application of the balloon model to the interpretation of BOLD transients. NeuroImage, 2004, 21, 144-153.	4.2	226
110	Efficiency, power, and entropy in event-related FMRI with multiple trial types. NeuroImage, 2004, 21, 387-400.	4.2	104
111	Efficiency, power, and entropy in event-related fMRI with multiple trial types. NeuroImage, 2004, 21, 401-413.	4.2	112
112	Trend detection via temporal difference model predicts inferior prefrontal cortex activation during acquisition of advantageous action selection. NeuroImage, 2004, 21, 733-743.	4.2	46
113	Coupling of cerebral blood flow and oxygen consumption during physiological activation and deactivation measured with fMRI. Neurolmage, 2004, 23, 148-155.	4.2	230
114	Modeling the hemodynamic response to brain activation. NeuroImage, 2004, 23, S220-S233.	4.2	1,023
115	Caffeine alters the temporal dynamics of the visual BOLD response. NeuroImage, 2004, 23, 1402-1413.	4.2	113
116	Increased diffusion sensitivity with hyperechos. Magnetic Resonance in Medicine, 2003, 49, 1098-1105.	3.0	8
117	Analysis and Design of Perfusion-Based Event-Related fMRI Experiments. NeuroImage, 2002, 16, 269-282.	4.2	40
118	Detection Power, Estimation Efficiency, and Predictability in Event-Related fMRI. NeuroImage, 2001, 13, 759-773.	4.2	251
119	Nonlinear temporal dynamics of the cerebral blood flow response. Human Brain Mapping, 2001, 13, 1-12.	3.6	183
120	Turbo ASL: Arterial spin labeling with higher SNR and temporal resolution. Magnetic Resonance in Medicine, 2000, 44, 511-515.	3.0	52